

A Method for Measuring the Surface Impedance of Superconductors in the Temperature Range 0.4–120 K

A. F. Shevchun and M. R. Trunin

Institute of Solid-State Physics, Russian Academy of Sciences, Chernogolovka, Moscow oblast, 142432 Russia
e-mail: shevchun@issp.ac.ru

Received March 14, 2006

Abstract—A method and a setup for making precision measurements of the temperature dependences of components of surface impedance $Z(T) = R(T) + iX(T)$ of small superconductor crystals in the temperature range 0.4–120 K have been developed. The setup combines a high-quality-factor resonance system for measuring the microwave response of a sample at a frequency of 28 GHz and a refrigerating unit with the use of evaporation of ^3He vapors. Measurements of $Z(T)$ of optimally doped $\text{YBa}_2\text{Cu}_3\text{O}_{6.93}$ single crystals in the superconducting and normal states were performed to illustrate the operation of the setup.

PACS numbers: 74.25.Nf, 07.57.Pt, 07.20.Mc

DOI: 10.1134/S0020441206050101

INTRODUCTION

Taking measurements of the temperature dependences of surface impedance $Z(T) = R(T) + iX(T)$ in absolute units at microwave frequencies $\omega = 2\pi f$ is one of the experimental methods for studying superconducting materials. The real part of the impedance—surface resistance $R(T)$ —is related to energy losses of an electromagnetic wave reflected from a superconductor. The imaginary part—reactance $X(T)$ —determines the nondissipating energy stored in the surface layer of the sample under study.

The requirements for the accuracy of microwave measurements became more stringent with the development of the physics of superconductors. Only precise microwave techniques allowed measurements of the dependence $Z(T)$ in classical superconductors with $T_c \leq 10$ K [1, 2] to be taken. These measurements were very informative: the value of energy gap Δ was found from temperature dependences of surface resistance $R(T) \sim e^{-\Delta/T}$ and reactance $X(T) \sim e^{-\Delta/T}$ at $T < T_c/2$; field penetration depth $\lambda(T)$ into a superconductor, from $X(T) = \omega\mu_0\lambda(T)$ at $T < T_c$; and the mean free path of electrons, from measurements of $R(T)$ and $X(T)$ in the normal state at $T \geq T_c$. In the case of local electrodynamics, the complex conduction of a superconductor can easily be found from impedance components measured in absolute units: $\sigma(T) = \sigma'(T) - i\sigma''(T) = i\omega\mu_0/Z^2(T)$. The possibility of applying the Bardeen–Cooper–Schrieffer (BCS) theory to explanation of the properties of classical superconductors was confirmed by a nonmonotonic behavior (a coherent peak) of the real part of microwave conductivity $\sigma'(T)$ observed at temperatures of $0.8 < T/T_c \leq 1$ [3, 4].

The issue of the accuracy of microwave measurements became more pressing after the advent of high-

temperature superconductors (HTSCs), in which high-quality single crystals are of small dimensions. One of the features of HTSCs is that their temperature dependence $Z(T)$ does not follow the BCS theory: instead of an exponential function at low temperatures, linear temperature dependences of both the surface resistance and the field penetration depth are observed [5], which are typical of superconductors with the d symmetry of the order parameter.

The method proposed in [6] is the most convenient for measuring the surface impedance of samples having surfaces no larger than ~ 1 mm². The main idea of this method is that a sample is placed on the end of a dielectric rod at the center of a cylindrical resonator operating on the H_{011} mode, i.e., into the region of an almost uniform magnetic microwave field. The resonator is evacuated in order to provide the possibility of varying the rod's temperature without changing the temperature of the resonator's walls. A sapphire rod is commonly used, because this material is characterized by a high thermal conductivity and weakly absorbs microwaves. By changing the rod's temperature and measuring the resonance frequency and Q factor of the resonator in the presence and absence of a sample, it is possible to determine the temperature dependences of both components of the sample's surface impedance.

The complexity of the experimental problem can be inferred from the example considered at the end of this paper. To measure the temperature dependence $Z(T)$ of an $\text{YBa}_2\text{Cu}_3\text{O}_{6.93}$ (YBCO) sample at a frequency $f = 3 \times 10^{10}$ Hz at $T < 30$ K, it is necessary to reliably record change $\Delta f = 100$ Hz in the resonance frequency at a change in the sample temperature of 1 K; i.e., $\Delta f/f \sim 10^{-9}$ (upon superconducting-to-normal-state transition of

the sample, the resonance frequency changed by 300 kHz).

The solution to this problem required the use of a high- Q resonator. First, we used a superconducting niobium resonator the walls of which were cooled with liquid ^4He from the outside. Its Q factor without a sample but with a sapphire rod placed inside it was $Q_0 = 1.8 \times 10^6$ at a temperature of the resonator's walls of $T = 4.2$ K. At $T = 1.4$ K, the Q factor was $Q_0 = 3.2 \times 10^6$. Second, a highly stable Agilent PSG-L E8244A generator with a frequency resolution of up to 0.1 Hz and an absolute stability no worse than 1 kHz/day was used. To preclude the effect of pickups from the supply line, the generator was powered through a voltage regulator. Measurements began several hours after the generator had been turned on. Third, a constant temperature of the resonator's walls to within an accuracy of 0.1 K was ensured during temperature changes of the rod with the sample. Evacuation of the resonator allowed $Z(T)$ measurements to be taken at temperatures of 0.4–120 K. A sample was cooled to temperatures below 2 K through evacuation of vapors of liquid ^3He by an external cryogenic pump [7]. A copper heat sink on which the sapphire rod was mounted was immersed directly into liquid ^3He .

DESCRIPTION OF THE SETUP

Figure 1 shows the part of the insert for the cryostat that is immersed into liquid ^4He . The insert is assembled from thin-walled (0.3–0.5 mm) stainless-steel tubes joined with argon welding to adapters and flanges from the same steel. The insert can conventionally be subdivided into two parts: a resonator unit and a sample-cooling unit.

Cylindrical niobium cavity resonator *I* constitutes the main part of the resonator unit. It is a cylinder with two caps. Its inner diameter and height are 14 mm. The H_{011} mode at a frequency $f = 28.2$ GHz was excited in the resonator. Since this is a degenerate mode with respect to the E_{111} mode, in order to suppress and shift E_{111} relative to H_{011} along the frequency axis, there are cylindrical protrusions with a diameter and height of 2.5 mm. Two holes with a diameter of 1.6 mm in the upper cap spaced by 7 mm are used to input microwave signals into and output from the resonator.

Two rectangular waveguides *3* with an internal cross section of 3.4×7.2 mm² that transmit microwave signals are placed in tube *2* and terminate in corner junctions (E -corner-type bents of the waveguide line). The short, 8-mm-long, sides of these corners are soldered to a brass washer supporting them. Holes drilled in the brass washer and corners coincide with the holes in the resonator's upper cap. Thin indium gaskets (not shown in Fig. 1) laid around these holes preclude the direct leakage of a microwave signal between the brass washer and the resonator's upper cap. Coupling elements *4*—coaxial waveguide with loops at their ends—

are inserted into the channels formed. The size of the coupling loops was selected experimentally: the total length of the central conductor is 7.5 mm, 3.5 mm of which belongs to the loop. Teflon parts of the coaxial waveguides are fixed in links *5* transforming the rotational motion of regulators, which are placed outside the cryostat at room temperature, into the translational motion of the coupling elements. The degree of coupling between the microwave channel and the resonator can be varied smoothly during an experiment by changing the distance between the loops and resonator.

The bottom cap of the resonator is pressed to its cylindrical part by bellows *6* serving as a spring. A 1-mm-diameter sapphire rod (*7*) enters the resonator through a 2-mm-diameter hole positioned at the center of the bottom cap. Sample *8* is fixed with Apiezon vacuum grease at the rod's upper end. RuO_2 thermometer *2* and heater *10* are attached to the part of the sapphire rod located outside the resonator. Six 0.05-mm-diameter manganin wires laid along thick-walled tube *11*, which ensures the rigidity of the structure, are connected to the thermometer and heater. The sapphire rod is glued into a copper holder, which is pressed to the end of copper rod *12* with a brass nut. A copper rod 10 mm in diameter and 110 mm in length is soldered to a collector of liquid ^3He (*13*).

Tube *2*, the inner parts of the waveguides and resonator, and the upper part of the copper rod constitute a common vacuum cavity, which is evacuated before the experiment through tube *11*. After the insert is cooled, the residual gas is frozen out and a high vacuum establishes in the cavity.

All dismantlable joints in the chain of components that includes flanges *I* and *II*, the cylindrical part of the resonator, and the flanges of parts *III* and *IV* are sealed hermetically with indium gaskets and clamped with brass bolts. To ensure access to the sapphire rod, the brass bolts joining the flanges of parts *III* and *IV* are unscrewed and the resonator unit suspended by tube *2* is lifted upward, while the sapphire rod, the resonator's bottom cap, and part *IV* remain at their places.

Being supplied to the sample-cooling unit, gaseous ^3He passes through 40- and 25-mm-diameter tubes *14* and *15*, respectively. When ^4He is evacuated from the cryostat's cavity, which is cooled to $T = 1.4$ K, gaseous ^3He condenses on the walls of these tubes. The condensate from tube *15* enters the collector of liquid ^3He and cools the copper rod. A vacuum jacket consisting of tubes *16* (30 mm in diameter and 80 mm in length), *17* (14 and 60 mm), *18* (18 and 50 mm), and *19* (80 and 80 mm) and upper and bottom caps is fastened to tube *15* with a silver solder. During its manufacture, the vacuum jacket was carefully evacuated to a high vacuum. To maintain vacuum at a low temperature, an adsorbent (activated carbon) is placed on the bottom cap.

The gaseous ^3He used in the sample-cooling unit is stored at room temperature in a 25-l vessel at a 0.6-atm pressure (Fig. 2). The amount of gas contained in the

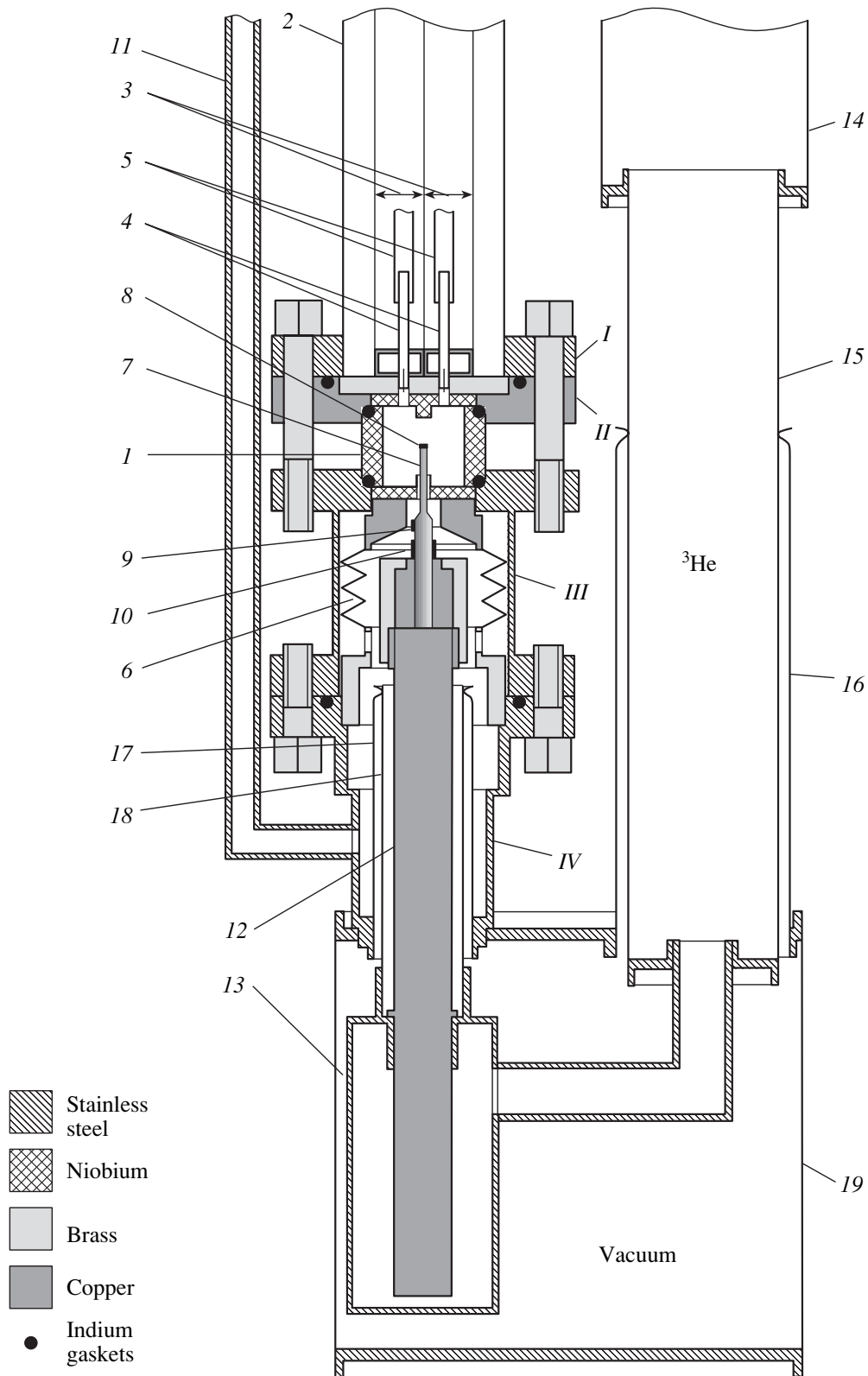


Fig. 1. Design of the insert's part placed inside the cryostat: (1) niobium resonator, (2) tube, (3) waveguides, (4) coupling elements, (5) links, (6) bellows, (7) sapphire rod, (8) sample, (9) thermometer, (10) heater, (11) thick-walled tube, (12) copper rod, (13) collector of liquid ^3He , (14, 15) ^3He -supplying tubes, (16–19) tubes of the vacuum jacket, and (I–IV) parts of the resonator unit.

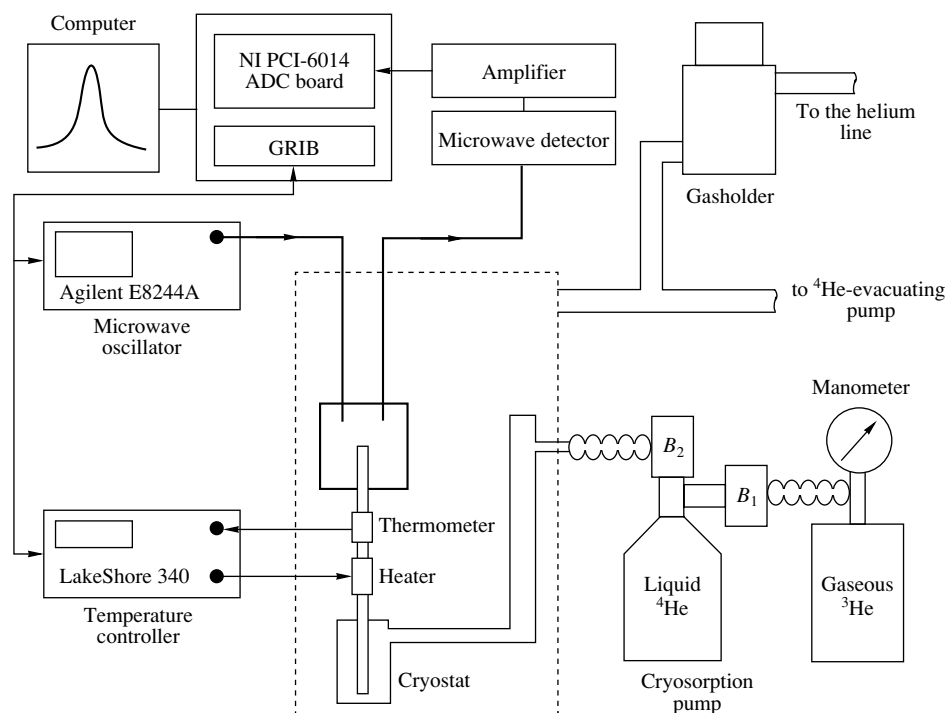


Fig. 2. Measurement diagram. V_1 and V_2 are valves.

vessel is monitored with a manometer. The vessel is joined to the cryogenic pump via a 10-mm-diameter bellows hose through valve V_1 . The pump is manufactured from a thin-walled stainless-steel tube 22 mm in diameter and 90 cm in length welded from below and filled with activated carbon as the sorbent. Copper radiators installed inside this tube improve the heat exchange between the sorbent and helium bath. An CTF-40 portable Dewar flask is used to cool the pump. The volume of the cryogenic pump is large enough to evacuate the entire ^3He contained in the insert. Valve V_2 mounted at the top of the pump is connected to the insert via a long flexible bellows hose 40 mm in diameter.

Because the resonator placed inside the cryostat is immersed in liquid ^4He , a change in the vapor pressure above the liquid leads to a change in the pressure on the resonator's walls, which in turn causes a change in the dimensions of the resonator. It has been ascertained experimentally that a change in the ^4He vapor pressure in the cryostat by 1 Torr leads to a change in the resonance frequency by 200 Hz. Therefore, to maintain a constant pressure $P \approx 1.05$ atm inside the cryostat, an oil gasholder having a volume of 50 l is used. As the gas fills the gasholder, the surplus amount of gas is discharged into the helium line.

Three operating temperature ranges of the setup can be distinguished:

(i) at temperatures of $5 < T < 120$ K, the vapor pressure above ^4He in the cryostat is maintained at a constant level with the gasholder;

(ii) at temperatures of $2 < T < 5$ K, gaseous ^4He is evacuated from the cryostat's cavity with a mechanical pump to a pressure of 2 Torr, which corresponds to a temperature of liquid ^4He of 1.4 K; and

(iii) at temperatures of $0.4 < T < 2$ K, gaseous ^4He condenses in the collector and is evacuated by the cryopump.

Evacuating ^4He vapors allows the temperature in the cryostat's cavity to be reduced from 4.2 to 1.4 K within 45 min; during this period, the entire amount of ^3He condenses in the collector. Evacuating ^3He vapors with cryosorption pump allows the temperature of the liquid to be lowered from 1.4 to 0.65 K within 2 min and from 0.65 to 0.5 K within 20 min. The operating time in this mode is 4 h. A further decrease in the temperature requires that the residual gas be removed from the cryopump and repeated evacuation be performed. As a result the temperature of ^3He falls from 0.5 to 0.4 K within 40 min.

According to the data from [8], the thermal conductivity of the sapphire rod 1 mm in diameter and 10 mm in length contained in the resonator is $\sim 1.5 \mu\text{W/K}$ at $T = 0.4$ K. This estimate imposes stringent limitations on the microwave power absorbed by a sample: a microwave power no higher than 100 nW must be dissipated in the resonator at $T < 1$ K.

THE MEASUREMENT CIRCUIT AND DATA PROCESSING

Figure 2 shows a block diagram of the automated system for measuring the temperature dependences of the Q factor and the resonance frequency.

The temperature of the sapphire rod is controlled with a LakeShore 340 controller that measures the resistance of the RuO₂ thermometer, which is installed on the sapphire rod, according to a four-probe circuit at a frequency of 20 Hz. Each measurement of the Agilent 82357A is recorded by a computer (PC) through a GPIB adapter, while the parameters of the proportional-integral-derivative temperature-regulating algorithm are inputted into the controller. A 300-Ω wire resistor attached to the sapphire rod serves as a heater.

Through the GPIB adapter, the PC specifies the frequency and power of the signal radiated by the Agilent PSG-L E8244A generator; this signal propagates along the waveguide and is fed to the resonator. A microwave transmitted through the resonator passes through a waveguide and falls on a measuring waveguide detector with a D-607 diode, which operates in the quadratic mode. The detector output signal passes through a laboratory amplifier with a gain of 5000 and arrives at the board of an NI PCI-6014 ADC, which inputs the measured voltage into the PC at a 200-kHz frequency and 16-bit resolution.

After the required temperature of the rod is set, the frequency dependence of the microwave power transmitted through the resonant system is recorded, as sweeping frequency f_{sw} of the generator-radiated signal is varied and the voltage across the diode is measured.

Measurements of the impedance of superconducting samples begin at a low temperature and are performed at minimum levels of coupling between the microwave line and the resonator, at which the maximum accuracy of low-loss measurements is attained. In this case, the frequency dependence of the microwave power transmitted through the resonance system has the form of an ordinary resonance curve:

$$P(f_{sw}) = \frac{Q_L^2 P_0}{4Q_L^2(f_0 - f_{sw})^2/f_0^2 + 1}, \quad (1)$$

where P_0 is a constant independent of frequency f_{sw} , f_0 is the resonance frequency, and Q_L is the quality factor of the resonance system. The accuracy attained in our measurements of a Q factor of $\sim 10^6$ was no worse than 1%, and the accuracy in determining the resonance frequency was ~ 20 Hz.

As the temperature approaches T_c , the energy loss in the sample increases and the Q factor of the resonance system decreases from 1.6×10^6 to 10^5 . In this case, as is seen from formula (1), the signal transmitted through the resonator decreases, thereby making it impossible to measure the dependence $P(f_{sw})$ at the same position of the loops in the sample's normal state. Therefore, the distance between the loops and the resonator is reduced

to a value that ensures a signal level sufficient for measurements at $T > T_c$.

If a substantial part of a coupling loop is in the resonator, the resonance curve observed cannot be described by formula (1). This is determined by the fact that the detector-registered microwave signal passes not only through the resonator but also through an additional channel—directly from one coupling loop to another. Assuming that, near the resonance peak in the resonance curve, the phase of a direct-penetration signal remains constant, the dependence of the microwave power arriving at the diode on frequency f_{sw} can be written in the form

$$P(f_{sw}) = \left| \frac{A_0}{2Q_L(f_0 - f_{sw})/f_0 + i} + B e^{i\phi} \right|^2, \quad (2)$$

where A_0 is the amplitude of the resonance signal and B and ϕ are the amplitude and phase of the direct-penetration signal, respectively.

The curves obtained under different coupling levels are joined via subtraction of constants $1/Q$ and Δf , which are temperature independent, as was purposefully checked, from the corresponding values of $1/Q_L(T)$ and $\Delta f(T)$ measured at large coupling values.

The temperature dependences of surface resistance $R(T)$ and reactance $X(T)$ for an isotropic sample can be found with the perturbation theory from the relationships [9]:

$$\begin{aligned} R(T) &= \Gamma [Q^{-1}(T) - Q_0^{-1}(T)]; \\ X(T) &= -\frac{2\Gamma}{f} [\Delta f(T) - \Delta f_0(T)] + X_0, \end{aligned} \quad (3)$$

where Γ is the sample's geometric factor and $Q_0(T)$ and $\Delta f_0(T)$ and $Q(T)$ and $\Delta f(T)$ are the temperature dependences of the Q factor and resonance frequency of the empty resonator and the resonator with a sample, respectively. For a typical YBCO sample at $T < 40$ K, the temperature-induced change in the Q factor for the empty resonator is $< 10\%$ of the change in the resonator's Q factor with a sample, and the temperature-induced change in the resonance frequency of the empty resonator is approximately half the change in the resonance frequency of the resonator containing a sample. The value of X_0 was found from the condition of the equality of the real and imaginary parts of the impedance in the normal state, $R(T) = X(T)$, because the criterion for the normal skin effect is satisfied for all samples studied in our experiments. The sample's geometric factor depends on the sample's shape, dimensions, and arrangement in the resonator. The issue of calculating the sample's geometric factor has been considered in detail in [9, 10].

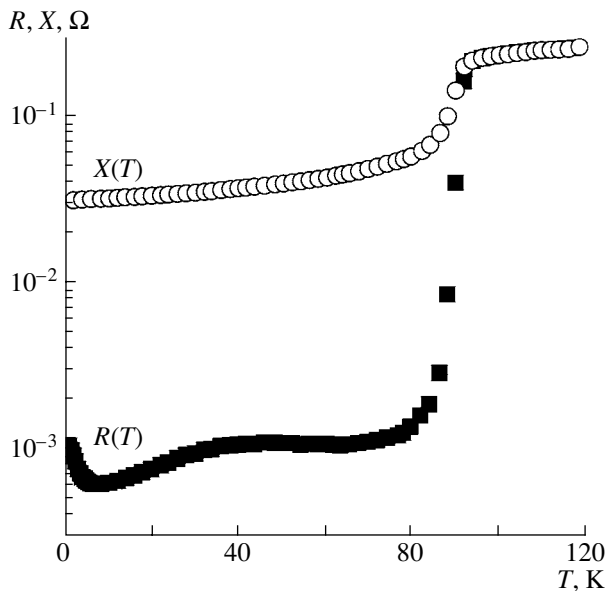


Fig. 3. Temperature dependences of surface resistance $R(T)$ and reactance $X(T)$ in the ab planes of a YBCO single crystal at a frequency of 28.2 GHz.

EXAMPLES OF EXPERIMENTAL RECORDS OF THE DEPENDENCE $Z(T)$ IN YBCO

An example of experimental temperature dependences of surface resistance $R(T)$ and reactance $X(T)$ of an optimally doped $\text{YBa}_2\text{Cu}_3\text{O}_{6.93}$ single crystal with a temperature of the superconducting transition $T_c = 92$ K is shown in Fig. 3. The crystal was grown with the technique of slow cooling from a solution in the melt with the use of a crucible made from barium zirconate BaZrO_3 [10] and had the shape of a plate measuring $0.5 \times 1.5 \times 0.1$ mm. Its geometric factor was $\Gamma = 9.5$ k Ω . The sample was mounted at the end of the sapphire rod so that the c axis was parallel to the microwave field; in this geometry, high-frequency currents flew in the ab crystal plane.

The adjustable coupling loops allowed our measurements to be performed in the sample's normal state at $92 < T \leq 120$ K and showed that the criterion for the normal skin effect is satisfied; i.e., $R(T) = X(T)$. The resistivity within this temperature range can be estimated from the formula $\rho(T) = 2R^2(T)/\omega\mu_0 \approx 0.6T$ $\mu\Omega$ cm.

In the superconducting state, the dependence $R(T)$ has a wide peak in the region $T \sim T_c/2$ typical of optimally doped YBCO crystals. Within the temperature range $10 < T < 40$ K, the dependences $R(T)$ and $\lambda(T) = X(T)/\omega\mu_0$ are linear (Fig. 4) and their extrapolation to $T = 0$ K yields values of the surface resistance of $R(0) \approx 0.5$ m Ω and the field penetration depth into cuprate planes of $\lambda(0) \approx 140$ nm.

The possibility of performing precise measurements at temperatures of $0.4 \leq T < 5$ K allowed an unusual behavior of the surface resistance to be revealed: $R(T)$ rapidly rises as the temperature decreases, while the

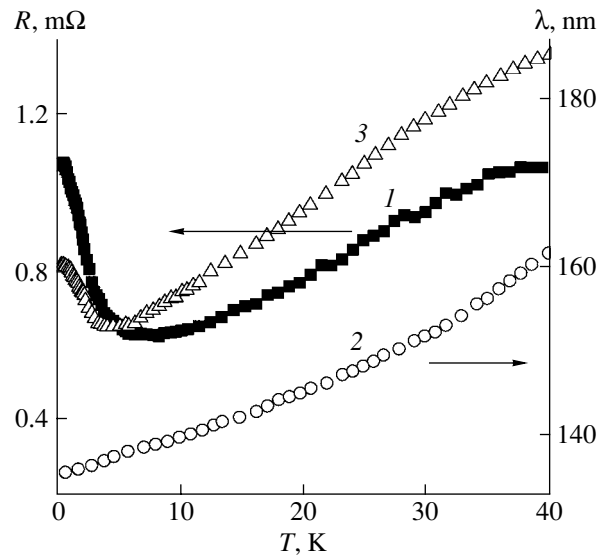


Fig. 4. Low-temperature parts of curves (1) $R(T)$ and (2) $\lambda(T) = X(T)/\omega\mu_0$ presented in Fig. 3; (3) behavior of $R(T)$ for another YBCO crystal from the same batch of samples.

temperature dependence of reactance $X(T)$ is linear to within the experimental accuracy. To verify this effect, we measured the surface impedance of another single crystal from the same batch of samples, which demonstrated a qualitatively identical behavior at low temperatures (see Fig. 4). At $T < 1$ K, the surface resistance tends to a constant value: $R(0.4 \text{ K}) = 1.06$ m Ω for the first and $R(0.4 \text{ K}) = 0.8$ m Ω for the second crystal.

An increase in the surface resistance at $T < 10$ K was observed earlier only in low-quality YBCO crystals with high values of surface resistance $R(0)$ [11] and in samples with Zn impurities, which lead to a significant decrease in critical temperature T_c [12]. Note that the rise of the dependence $R(T)$ was accompanied by an increase in penetration depth $\lambda(T)$ so that a minimum in curves $\lambda(T)$ was observed in a region of 4–7 K.

It is known that the low-temperature features in $\lambda(T)$ in HTSCs characterized by an anisotropic d -symmetric order parameter, a coherence length of $\xi_0 \sim 1$ nm, and $\lambda_0 = \lambda(0) \sim 100$ nm in the ab planes can be displayed at two temperatures: $T^* \sim (\xi_0/\lambda_0)T_c \sim 1$ K [13] and $T_m \sim (\xi_0/\lambda_0)^{0.5}T_c \sim 10$ K [14]. Temperature T^* corresponds to a nonlocality-caused crossover from a linear to quadratic dependence $\Delta\lambda(T)$, and T_m corresponds to the paramagnetic contribution from the surface bound states into $\Delta\lambda(T)$ that increases, as the temperature decreases.

Pronounced minima in the curves $R(T)$ and $\lambda(T)$ at $T \sim 5$ K and their rise at $T < 5$ K were also observed in GdBaCuO [15] and NdCeCuO crystals [16], the low-temperature volumetric paramagnetism of which is evidently ensured by Gd and Nd magnetic ions.

No peculiarities in the curves $\lambda(T)$ are observed in Fig. 4 to within an error of measuring the field penetration depth into the sample, $\Delta\lambda(T) \leq 1$ nm. This result agrees with the presence of too few bound states with a zero energy in the orientation of the YBCO crystal relative to the microwave magnetic field used in our experiments; these states are needed to form a minimum in the curve $\lambda(T)$ at $T \approx T_m$ [14].

Hence, an increase in surface resistance $R(T) = \omega^2 \mu_0^2 \lambda^3 \sigma'(T)/2$ at $T < 10$ K can be determined only by an abrupt increase in the real part of conductivity $\sigma'(T)$, which is $\sigma'(T) = n_n(T)\tau(T)e^2/[m(1 + \omega^2\tau^2)]$ in the two-fluid model, where n_n is the fraction of normal carriers and τ is the quasi-particle relaxation time for impurities, which is 10^{-11} s ($\hbar/(\tau k_B) \approx 5$ K) in YBCO crystals at $T \ll T_c$ [17, 18]. In d -symmetric superconductors with the maximum value of the slit Δ_0 , quasi-particles are excited thermally near the slit's zeros at $\Delta_0 \gg T > \hbar/(\tau k_B)$, but all of the known mechanisms of quasi-particle scattering by point or extended defects lead to a decrease in the conductivity, $\sigma'(T) \rightarrow 0$, at $T \rightarrow 0$ but not to its increase [18, 19]. At the same time, the presence of impurities in a d -type superconductor leads to a finite density of quasi-particles at $T = 0$ owing to the localization effects. These quasi-particles are scattered by the same impurities, thereby ensuring nonzero conductivity $\sigma'(0) \neq 0$ at $T < \hbar/(\tau k_B)$ [20]. It has not been determined how $\sigma'(T)$ changes upon change from the thermal regime ($T > \hbar/(\tau k_B)$) to the disorder regime ($T < \hbar/(\tau k_B)$).

CONCLUSIONS

A new setup for precise measurements of real $R(T)$ and imaginary $X(T)$ parts of the surface impedance of superconducting crystals at millimeter waves and temperatures of $0.4 \leq T \leq 120$ K has been designed. The block diagram and the procedure for determining the numerical values of $R(T)$ and $X(T)$ from the resonator's Q factor and the resonance-frequency shift, which are obtained in direct measurements, are described. The dependences $R(T)$ and $X(T)$ measured for an optimally doped $\text{YBa}_2\text{Cu}_3\text{O}_{6.93}$ single crystal demonstrate the known temperature behavior of the impedance of such crystals in the range $5 < T \leq 120$ K. A new effect—a considerable increase in $R(T)$, the nature of which remains unclear—has been discovered at $T < 5$ K.

ACKNOWLEDGMENTS

We are grateful to V.F. Gantmakher for his help in the work with this paper, G.V. Merzlyakov and

S.V. Ryzhkov for their engineering assistance, and Yu.A. Nefedov and Yu.S. Barash for useful discussions.

This study was supported in part by the Russian Foundation for Basic Research (projects no. 04-02-17358 and 06-02-17098) and the scientific programs of the Russian Academy of Sciences.

REFERENCES

1. Khaikin, M.S., *Dokl. Akad. Nauk SSSR*, 1950, no. 75, p. 661.
2. Turneaure, J.P., Halbritter, J., and Schwettman, H.A., *J. Supercond.*, 1991, vol. 4, p. 341.
3. Klein, O., Nicol, E.J., Holczer, K., et al., *Phys. Rev. B*, 1994, vol. 50, p. 6307.
4. Trunin, M.R., Zhukov, A.A., and Sokolov, A.T., *Zh. Eksp. Teor. Fiz.*, 1997, vol. 111, p. 696 [*JETP* (Engl. Transl.), vol. 84, p. 383].
5. Hardy, W.N., Bonn, D.A., Morgan, D.C., et al., *Phys. Rev. Lett.*, 1993, vol. 70, p. 3999.
6. Sridhar, S. and Kennedy, W.L., *Rev. Sci. Instrum.*, 1988, vol. 54, p. 531.
7. Dorozhkin, S.I., Zverev, V.N., and Merzlyakov, G.V., *Prib. Tekh. Eksp.*, 1996, no. 2, p. 165.
8. Lounasmaa, O.V., *Experimental Principles and Methods Below One Degree Kelvin*, New York: Academic, 1974. Translated under the title *Printsipy i metody polucheniya temperatur nizhe 1 K*, Moscow: Mir, 1977, p. 288.
9. Trunin, M.R., *Usp. Fiz. Nauk*, 1998, vol. 168, no. 9, p. 931 [*Phys. Usp.* (Engl. Transl.), vol. 41, no. 9, p. 843].
10. Nefyodov, Yu.A., Trunin, M.R., Zhohov, A.A., et al., *Phys. Rev. B*, 2003, vol. 67, p. 144504.
11. Jacobs, T., Sridhar, S., Rieck, C.T., et al., *J. Phys. Chem. Solids*, 1995, vol. 56, p. 1945.
12. Bonn, D.A., Kamal, S., Bonakdarpour, A., et al., *Czech. J. Phys.*, 1996, vol. 46, p. 3195.
13. Kosztin, I. and Legget, A.J., *Phys. Rev. Lett.*, 1997, vol. 79, p. 135.
14. Barash, Yu.S., Kalenkov, M.S., and Kurkijarvi, J., *Phys. Rev. B*, 2000, vol. 62, p. 6665.
15. Gough, C.E., Ormeno, R.J., Hein, M.A., et al., *J. Supercond.*, 2001, vol. 14, p. 73.
16. Prozorov, R., Giannetta, R.W., Fournier, P., and Greene, R.L., *Phys. Rev. Lett.*, 2000, vol. 85, p. 3700.
17. Hosseini, A., Harris, R., Kamal, S., et al., *Phys. Rev. B*, 1999, vol. 60, p. 1349.
18. Trunin, M.R. and Golubov, A.A., in *Spectroscopy of High-Tc Superconductors. A Theoretical View*, Plakida, N.M., Ed., London, New York: Taylor and Francis, 2003, pp. 159–233.
19. Durst, A.C. and Lee, P.A., *Phys. Rev. B*, 2002, vol. 65, p. 094501.
20. Lee, P.A., *Phys. Rev. Lett.*, 1993, vol. 71, p. 1887.